New Phytologist

Research

Divergence times and the evolution of morphological complexity in an early land plant lineage (Marchantiopsida) with a slow molecular rate

Juan Carlos Villarreal A.[1,3,4], Barbara J. Crandall-Stotler[2], Michelle L. Hart[1], David G. Long[1] and Laura L. Forrest[1]

[1]Royal Botanic Gardens Edinburgh, 20A Inverleith Row, Edinburgh, EH3 5LR, UK; [2]Department of Plant Biology, Southern Illinois University, Carbondale, IL 62901, USA; [3]Present address: Smithsonian Tropical Research Institute, Ancón, 0843-03092 Panama, Republic of Panama; [4]Present address: Département de Biologie, Université Laval, Québec, Canada G1V 0A6

Authors for correspondence:
Juan Carlos Villarreal A
Tel: +1418 656 3180
Email: jcarlos.villarreal@gmail.com

Laura L. Forrest
Tel: + 44(0) 131248 2952
Email: L.Forrest@rbge.ac.uk

Received: *29 June 2015*
Accepted: *15 September 2015*

New Phytologist (2015)
doi: 10.1111/nph.13716

Key words: ancestral character reconstruction, diversification, gas exchange, liverworts, *Marchantia*, slow molecular rate.

Summary

- We present a complete generic-level phylogeny of the complex thalloid liverworts, a lineage that includes the model system *Marchantia polymorpha*. The complex thalloids are remarkable for their slow rate of molecular evolution and for being the only extant plant lineage to differentiate gas exchange tissues in the gametophyte generation. We estimated the divergence times and analyzed the evolutionary trends of morphological traits, including air chambers, rhizoids and specialized reproductive structures.
- A multilocus dataset was analyzed using maximum likelihood and Bayesian approaches. Relative rates were estimated using local clocks.
- Our phylogeny cements the early branching in complex thalloids. *Marchantia* is supported in one of the earliest divergent lineages. The rate of evolution in organellar loci is slower than for other liverwort lineages, except for two annual lineages. Most genera diverged in the Cretaceous. *Marchantia polymorpha* diversified in the Late Miocene, giving a minimum age estimate for the evolution of its sex chromosomes. The complex thalloid ancestor, excluding Blasiales, is reconstructed as a plant with a carpocephalum, with filament-less air chambers opening via compound pores, and without pegged rhizoids.
- Our comprehensive study of the group provides a temporal framework for the analysis of the evolution of critical traits essential for plants during land colonization.

Introduction

The fossil occurrence of cryptospore dyad and tetrad assemblages signals the formation of a terrestrial flora *c.* 450 million yr ago (Wellman *et al.*, 2003; Brown *et al.*, 2015). Bryophytes (hornworts, liverworts and mosses) are generally accepted as the first divergences in extant embryophyte phylogeny and, as such, may hold morphological and genomic clues to the understanding of the evolutionary pressures faced by early land colonizers. Although the branching pattern of the early land plant lineages remains unresolved (Wicket *et al.*, 2014), the most widely accepted topology recovers liverworts as the sister group to all other embryophytes (Qiu *et al.*, 2006). Liverworts include *c.* 5000 species in three classes: Haplomitriopsida (*c.* 17 spp.), Marchantiopsida (complex thalloid clade, *c.* 340 spp.) and Jungermanniopsida (simple thalloid and leafy clades, > 4000 spp.). The complex thalloid liverworts have a strikingly slow DNA substitution rate (*rbc*L, Lewis *et al.*, 1997) in contrast with the other two classes, Haplomitriopsida and Jungermanniopsida (Fig. 1), but, nonetheless, display substantial morphological diversity among genera.

The complexity of the complex thalloids, a group including the model system organism *Marchantia polymorpha* L., derives from the layered anatomy of the thalloid gametophyte, which is usually differentiated into a dorsal, non-chlorophyllose epidermis, an upper photosynthetic, assimilatory zone, a parenchymatous, non-photosynthetic storage zone and a ventral epidermis that bears rows of scales and two types of rhizoid (Fig. 1c). In most genera, the assimilatory zone contains abundant, schizogenously derived air chambers that are confluent with epidermal pores (Barnes & Land, 1907). However, Marchantiopsida diversity encompasses plants with simple, undifferentiated thalli (Blasiales), as well as a large number of air chamber-bearing xerophytic species with either desiccation avoidance or tolerance strategies (e.g. *Plagiochasma*, *Riccia*) and weedy species such as *Lunularia cruciata* and *M. polymorpha* (Fig. 1b). *Marchantia polymorpha* is a flagship species for the complex thalloids; its ease of cultivation, gene targeting, the fully sequenced male sex chromosome and abundant genomic resources have been instrumental to its pioneering as the new model for synthetic and evolutionary biology (Yamato *et al.*, 2007; Ishizaki *et al.*, 2013a,b; Bowman, 2015; Saint-Marcoux *et al.*, 2015).

In the complex thalloid lineage, there are three major morphological innovations: (1) internalized air chambers that are schizogenously derived from epidermal initials and open via a pore; (2) dimorphic rhizoids, that is, specialized 'pegged' rhizoids

© 2015 Royal Botanic Garden Edinburgh
New Phytologist © 2015 New Phytologist Trust

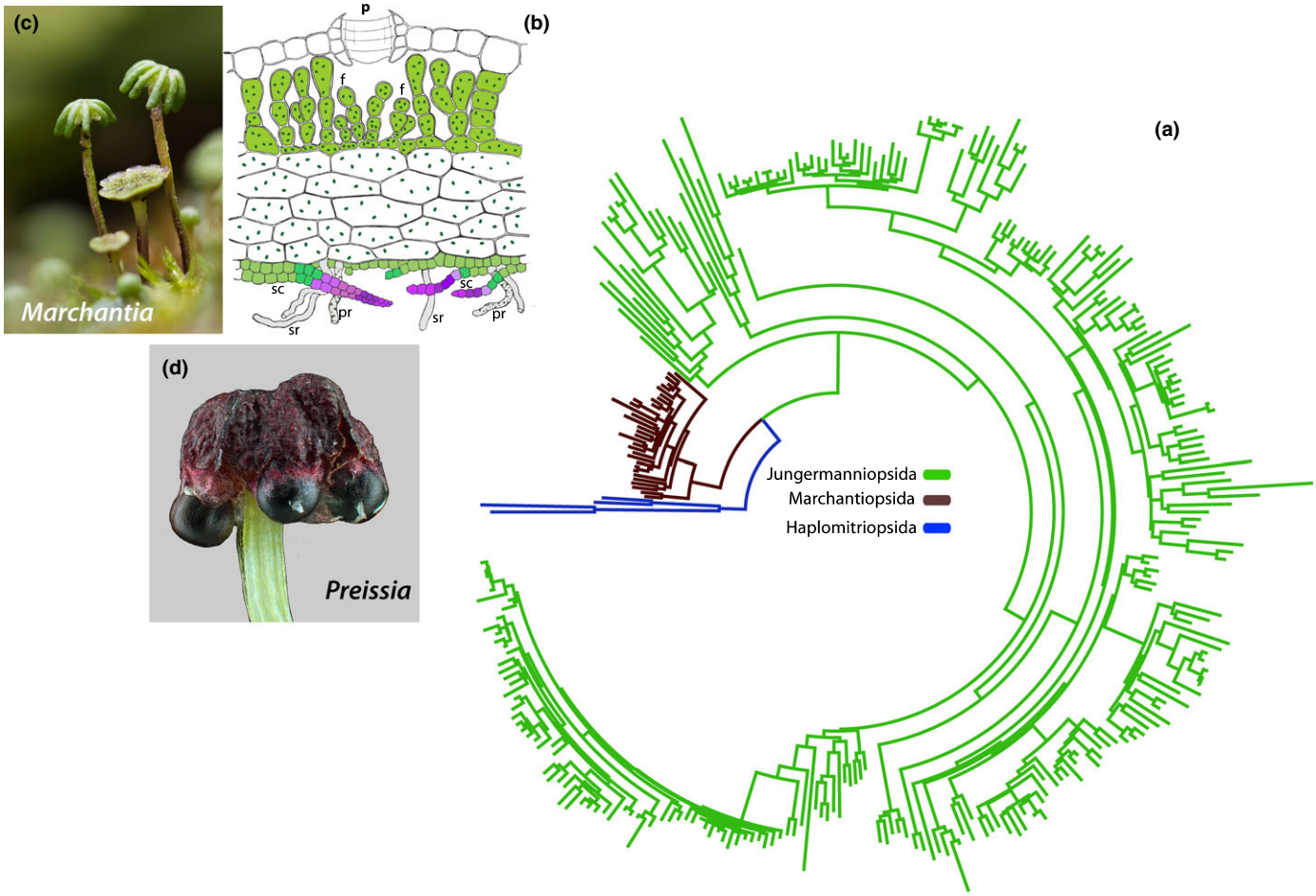

Fig. 1 (a) Maximum likelihood tree of 303 liverwort genera, covering over 80% of the total extant diversity, based on 6820 aligned nucleotides from five plastid (*atp*B, *psb*A, *psb*T, *rbc*L and *rps*4) and two mitochondrial (*rps*3 and *nad*1) loci (data from Laenen *et al.*, 2014), re-analyzed in RAxML to include only coding regions of the organellar loci (treebase number: 18277). The Marchantiopsida, or complex thalloids (*c.* 340 species, in brown), have very short branches in comparison with the early divergent Haplomitriopsida (*c.* 17 species, in blue) and the mega-diverse simple thalloid and leafy liverworts, Jungermanniopsida (*c.* 4000 species, in green). (b) Transverse section of mature thallus of a typical *Marchantia*, with an assimilative layer opening to a complex pore (p). The chamber is lined with photosynthetic filaments (f). The ventral part of the thallus has ventral scales (sc) and two types of rhizoid: smooth (sr) and pegged (pr). Drawing licensed by Florida Center for Instructional Technology (ID 23468) and modified by O. Pérez. (c) *Marchantia polymorpha*, showing stalked reproductive structures: two carpocephala (umbrella-like structures that carry archegonia and eventually sporophytes) from one plant and a nearby antheridiophore from another plant. (d) Carpocephalum of *Preissia quadrata* with four sporophytes, the carpocephalum showing air pores. Credits: (c) J. Bechteler; (d) D. Callaghan.

in addition to the smooth rhizoids that are present in most other liverwort groups; and (3) the elevation, in most genera, of archegonial receptacles on specialized thallus branches, known as archegoniophores (= carpocephala after fertilization) (Fig. 1). The archegoniophore/carpocephalum complex can contain air chambers and pores, with rhizoids that may grow down through furrows in the stalk to connect the receptacles to groundwater, whilst the receptacles themselves contain several archegonia, and subsequently sporophytes (Schuster, 1992; Fig. 1b,d). The first two innovations are presumably related to photosynthesis and water economy, whereas the specialized female reproductive structures are associated with the enhancement of spore dispersal (Schuster, 1992; Bischler, 1998; Duckett *et al.*, 2014).

Here, based on a complete generic phylogeny (*c.* 24% of the 330–340 species and all 36 genera of complex thalloids), a large molecular dataset (*c.* 15 000 bp) and a fossil-calibrated timetree, we address the morphological and molecular evolution of the complex thalloids to settle controversial phylogenetic relationships within the group (He-Nygren *et al.*, 2004;. Forrest *et al.*, 2006; Laenen *et al.*, 2014). Our five main questions are: (1) what is the branching pattern among early divergent lineages of complex thalloids?; (2) when did the main clades of complex thalloid liverworts diverge?; (3) is the rate of molecular evolution constant across complex thalloids?; (4) what is the timing of the origin of *Marchantia polymorpha*?; and (5) how did morphological complexity evolve within Marchantiopsida?

Materials and Methods

Molecular methods

We sequenced 111 accessions representing 76–79 complex thalloid species, corresponding to all 36 genera, and 13 outgroup taxa selected, based on a previous phylogenetic analysis (Forrest *et al.*,

© 2015 Royal Botanic Garden Edinburgh
New Phytologist © 2015 New Phytologist Trust

2006), from the two other liverwort classes (Table 1). Voucher information and GenBank accession numbers are available in Supporting Information Table S1. DNA extraction and PCR amplification followed standard protocols (Table S2). The dataset included nucleotide sequences from 11 loci (14 829 bp): part of the nuclear large ribosomal subunit (26S); mitochondrial regions *nad*1, *nad*5 and *rps*3; plastid regions *atp*B, *psb*T-*psb*N-*psb*H, *rbc*L, cpITS, *rpo*C1, *rps*4 and *psb*A. We used Geneious 5.6.6 (Biomatters Ltd, Auckland, New Zealand) to align the nucleotide sequences, with the resulting alignment manually improved on the basis of the *Marchantia* plastid and mitochondrial genomes (Ohyama *et al.*, 1986; Oda *et al.*, 1992). A subset of the matrix, hereafter called the reduced dataset, contained 76 taxa and included a single representative per species. This was used for ancestral reconstruction and dating analyses (see Molecular clock dating). Trees for the reduced data matrix were rooted on Blasiales (*Blasia pusilla* and *Cavicularia densa)*, the sister clade to all other complex thalloids (Forrest *et al.*, 2006).

Phylogenetic analyses

We used PartitionFinder (Lanfear *et al.*, 2010) to obtain the optimal data partition scheme (by locus) and the associated nucleotide substitution models, resulting in seven partitions. The dataset was analyzed under the maximum likelihood (ML) criterion using RaxML black box (Stamatakis *et al.*, 2008) with 100 bootstrap replicates (MLB). Bayesian analyses were conducted in MrBayes 3.2 (Ronquist *et al.*, 2012) using the default two runs and four chains, with default priors on most parameters. Model parameters for state frequencies, the rate matrix and gamma shape were unlinked, and posterior probabilities (PPs) of tree topologies were estimated from both partitions. Burn-in and convergence were visually assessed using Tracer 1.5 (Rambaut *et al.*, 2014). Stationarity and convergence of the chains were usually achieved in MrBayes after 2.5×10^6 generations, with trees sampled every 5000th generation for a total length of 20×10^6 generations to avoid trees being stuck in a suboptimal tree landscape; we discarded 25% of each run and then pooled the runs. The final matrix is available at TreeBase study 18277.

Molecular clock dating

We ran a series of analyses using an internal fossil, with the root constrained using a secondary calibration from previous studies and following the best recommended practices for dating analyses (Newton *et al.*, 2007; Cooper *et al.*, 2012; Parham *et al.*, 2012; Warnock *et al.,* 2012; Feldberg *et al.*, 2014). The fossil is placed near the root, which simulation studies show to improve the accuracy of age estimates (Duchêne *et al.*, 2014).

The earliest reliable complex thalloid fossils are found in Upper Triassic and Cretaceous sediments (Anderson, 1976; Li *et al.*, 2014). Several fossils, such as *Naiadita lanceolata* and *Blasiites lobatus*, have been assigned to the crown groups of complex thalloids. However, their unusual features make their assignment to any order of extant liverworts ambiguous (Heinrichs *et al.*, 2007; Katagiri & Hagborg, 2015). We used *Marchantites cyathodoides* (Townrow) H. M. Anderson, based on specimen number 13929, housed in the South African Museum, Cape Town from the Upper Umkomaas, Molteno Formation, Karroo Basin, South Africa (Townrow, 1959; Anderson, 1976; H. M. Anderson, pers. comm.) (Carnian, Upper Triassic, 237 million yr ago (Ma) ± 1 Ma to 228.4 Ma ± 2 Ma, Ogg, 2012). The fossil thallus has a midrib and reduced air chambers with pores, on the dorsal surface, similar to extant genus *Cyathodium* (Townrow, 1959), but has smooth rhizoids with both thick and thin walls

Table 1 Orders and genera of taxa used in this study, with an approximate species number (Söderström *et al.*, in press)

Subclass – Order	Family	Genus, accepted species and species sampled for this study
Blasiidae		
Blasiales	Blasiaceae	*Blasia (1/1)*, *Cavicularia (1/1)*
Marchantiidae		
Neohodgsoniales	Neohodgsoniaceae	*Neohodgsonia (1/1)*
Sphaerocarpales	Sphaerocarpaceae	*Geothallus (1/1)*
	Monocarpaceae	*Monocarpus (1/1)*
	Sphaerocarpaceae	*Sphaerocarpos 7/3*
Riellales	Riellaceae	*Austroriella (1/1)*, *Riella (20/1)*
Lunulariales	Lunulariaceae	*Lunularia (1/1)*
Marchantiales	Exormothecaceae	*Aitchisoniella (1/1)*, *Exormotheca (7/2)*, *Stephensoniella (1/1)*
	Aytoniaceae	*Asterella (46/12)*, *Cryptomitrium (3/2)*, *Mannia (8/4)*, *Plagiochasma (16/3)*, *Reboulia (1/1)*
	Marchantiaceae	*Bucegia (1/1)*, *Marchantia (36/9)*, *Preissia (1/1)*
	Cleveaceae	*Athalamia (1/1)*, *Clevea (3/1)*, *Peltolepis (2/1)*, *Sauteria (2/2)*
	Conocephalaceae	*Conocephalum (3/3)*
	Corsiniaceae	*Corsinia (1/1)*, *Cronisia (2/2)*
	Cyathodiaceae	*Cyathodium (11/4)*
	Dumortieraceae	*Dumortiera (1–3/1–3)*
	Monocleaceae	*Monoclea (2/2)*
	Monosoleniaceae	*Monosolenium (1/1)*
	Oxymitraceae	*Oxymitra (2/1)*
	Ricciaceae	*Riccia (154/4)*, *Ricciocarpos (1/1)*
	Targioniaceae	*Targionia (3/1)*
	Wiesnerellaceae	*Wiesnerella (1/1)*
Outgroup		
Treubiales	Treubiaceae	*Apotreubia (4/1)*, *Treubia (6/2)*
Calobryales	Haplomitriaceae	*Haplomitrium (7/2)*
Metzgeriales	Metzgeriaceae	*Metzgeria (c. 100/1)*
Pallaviciniales	Pallavicinaceae	*Pallavicinia (15/1)*
Pelliales	Pelliaceae	*Pellia (8/1)*
Pleuroziales	Pleuroziaceae	*Pleurozia (11/1)*
Ptilidiales	Ptilidiaceae	*Ptilidium (3/1)*

© 2015 Royal Botanic Garden Edinburgh
New Phytologist © 2015 New Phytologist Trust

(similar to the dimorphic rhizoids of *Neohodgsonia*), and one row of ventral scales along the midrib. Its features are shared by most complex thalloids (excluding Blasiales), and so the fossil was used to constrain the stem node of *Neohodgsonia* and the remaining complex thalloids. A minimum age constraint was enforced by applying a uniform prior from the fossil age to 450 Ma (a conservative root age based on previous studies) (Newton *et al.*, 2007; Cooper *et al.*, 2012; Feldberg *et al.*, 2014; see later).

Second, we used a normal distribution around the root, with mean (in real time) of 270 Ma and SD of 60 Ma applied to the root, with a minimum age of 250 Ma and a maximum age of 450 Ma. The mean age was obtained from Feldberg *et al.* (2014) in their study of the diversification of leafy liverworts, which lacked a calibration for complex thalloids; this study only provided a point estimate for the node at 270 Ma (their Supporting Information 2). The uncertainty around the age was modeled using a truncated normal distribution to include the lower interval of the dates recovered for Marchantiopsida in Newton *et al.* (2007) in their study of moss diversification (their Table 17.2). The maximum age of the constraint is probably an overestimate, and is beyond the oldest age published for this node using fewer taxa and loci (Newton *et al.*, 2007; Cooper *et al.*, 2012).

To explore the effective priors, we ran an analysis with an empty alignment to compare the frequency distribution of age estimates for each calibrated node with the prior. The *Marchantites cyathodoides* calibration has its 95% highest posterior density (HPD) between 226 and 348 Ma, with a median age of 270 Ma, slightly older than the fossil calibration, but not in full disagreement with the original priors (Fig. S1). The root prior is abutted to the constraint age with its HPD from 250 to 377 Ma and a median age of 300 Ma. The posteriors and topology from the empty alignment departed from the priors, indicating that our dataset is informative.

Bayesian divergence time estimation used a Yule tree prior and the GTR + Γ substitution model with unlinked data partitions to account for the mitochondrial, nuclear and plastid data. A pilot analysis using the seven-partitioned dataset suggested by PartitionFinder failed to initiate the run; therefore, we chose a simpler partition scheme, by genome. The analyses used an uncorrelated log-normal (UCLN) relaxed clock model. Markov chain Monte Carlo (MCMC) chains were run for 500 million generations, with parameters sampled every 50 000th generation. Tracer 1.5 (Rambaut *et al.*, 2014) was used to assess effective sample sizes (ESSs) for all estimated parameters and to decide appropriate burn-in percentages. We verified that all ESS values were > 200. Trees were combined in TreeAnnotator 1.8 (Beast package; Drummond *et al.*, 2012), and maximum clade credibility trees with mean node heights were visualized using FigTree 1.4.0 (Rambaut, 2014). We report HPD intervals (the interval containing 95% of the sampled values). Absolute rates for each genomic partition were estimated using the formula $\sum_i b_i / \sum_i t_i$, where t_i is the time units of the ith branch and r_i is the rate of the ith branch, $b_i = r_i\ t_i$ is the branch length in substitutions per site, automated in the Beast package and Tracer.

Rate heterogeneity

Rate heterogeneity in the complex thalloid dataset was assessed to detect any change in rate within the clade, using Beast v.1.8 (Drummond *et al.*, 2012). Two analyses were conducted: one with UCLN and another with local clocks (LCs) (Drummond & Suchard, 2010). The three-partitioned dataset was used for the analyses, with a Yule tree prior, the substitution parameters and clock parameters unlinked across partitions, and topologies were linked. Tracer 1.6 was used to assess ESS for all estimated parameters and to decide appropriate burn-in percentages. We verified that all ESS values were > 200. Each analysis was run for 500 million generations, with the chain sampled every 25 000th generation. The LC analyses converged after 250 million generations; ESS values above 200 were recovered for nearly all parameters. Trees were combined in TreeAnnotator 1.8 and maximum clade credibility trees with mean node heights were visualized using FigTree 1.4. All analyses were run using the CIPRES Science Gateway servers (Miller *et al.*, 2010).

Ancestral reconstruction of complex traits

Based on a detailed study of character evolution in Marchantiidae (Bischler, 1998) and our personal observations, we scored five morphological characters that were used to define extant lineages of complex thalloids. The binary characters were: (1) presence/absence of carpocephala; (2) presence/absence of pegged rhizoids; (3) presence/absence of thallus epidermal pores; (4) presence/absence of air chambers; and (5) presence/absence of photosynthetic filaments. In addition, (3) and (4) were broken down into four and five states, respectively (Table 2). The additional scoring of thallus and carpocephalum pore type and air chamber type was conducted to test whether the different complex traits show a phylogenetic pattern within the group. The coding for pore type and air chamber type follows Tables 3 and 4 of Bischler (1998), and has been verified for lineages excluded from her study. Unlike Bischler's study, we included *Monoclea* and Sphaerocarpales as ingroup taxa, and rooted the analyses on Blasiales.

The coding for thallus pore type is: 0 = absent or vestigial; 1 = simple opening in epidermal cells; 2 = simple, one ring of cells, inner ring of collapsed cells present or absent; 3 = simple, several concentric rings of cells, inner ring of collapsed cells present; 4 = compound, several concentric rings of cells, inner ring of collapsed cells present.

The coding for carpocephalum pore type is: 0 = not applicable (carpocephalum absent); 1 = pores absent or vestigial; 2 = simple pores; 3 = compound pores.

The coding for assimilative layer type is: 0 = no distinct layer or layer without air chambers; 1 = one layer of air chambers, no chlorophyllose filaments; 2 = several layers of air chambers in central part of thallus, air chambers with or without a pore, no chlorophyllose filaments; 3 = one layer of air chambers, floor with chlorophyllose filaments (at least rudimentary), each chamber with one pore.

To reconstruct the ancestral traits of complex thalloids, we optimized the binary traits of major lineages of extant complex

© 2015 Royal Botanic Garden Edinburgh
New Phytologist © 2015 New Phytologist Trust

Table 2 Proportional likelihood associated with the reconstruction of trait evolution for two competing explicit evolutionary models (see the text for details) in complex thalloids

			Nodes of interest – proportional likelihood for state 1									
Trait	State		Node 1	Node 2	Node 3	Node 4	Node 5	Node 6	Node 7	Node 8	Node 9	Node 10
Carpocephala	Absent (0)	Present (1)	0.68	0.78	0.90	0.26	0.99	0.99	0.99	0.99	0.06	0.01
Pegged rhizoids	Absent (0)	Present (1)	0.14	0.16	0.77	0.06	0.99	0.99	0.99	0.99	0.009	0.99
Air pores	Absent or vestigial (0)	Present (1)	0.66	0.76	0.88	0.23	0.99	0.99	0.99	0.99	0.99	0.99
Photosynthetic layer	Absent or indistinct (0)	Present (1)	0.66	0.76	0.88	0.23	0.99	0.99	0.98	0.99	0.99	0.99
Photosynthetic filaments	Absent (0)	Present (1)	0.45	0.56	0.84	0.14	0.919	0.99	0.94	0.50	0.27	0.29

The reconstructions employ the chronogram obtained from BEAST, using an asymmetrical two-parameter Markov model.

thalloids onto a Bayesian chronogram from the reduced dataset. Ancestral reconstruction relied on ML as implemented in Mesquite using the Markov one- or two-parameter models (Maddison & Maddison, 2010) for binary traits. To test the null hypothesis of equal transition frequencies between the characters, we performed a likelihood ratio test (LRT) that compared the likelihood of a one-parameter model of equal transition rates (called q) with a two-parameter, asymmetric model, which allows separate rates of transitions to characters (Pagel, 1999). Test significance was evaluated on the basis of a χ^2 distribution with one degree of freedom. To test for associations between the five binary traits, we used an ML approach in the discrete module of Mesquite (Maddison & Maddison, 2010). Pairs of traits were analyzed successively, using two models: a four-rate model describing independent evolution of traits, and an eight-rate model describing correlated evolution. The tests showed no correlation between traits and no further results are reported here. Finally, a parsimony analysis was conducted to reconstruct ancestral multistate traits (> two states).

Results

Molecular analyses

The complete complex thalloid matrix of 111 taxa consists of 14 829 aligned nucleotides, with 10 540 included characters, 2807 of which are parsimony informative. The reduced data matrix (76 taxa) consists of 12 260 included characters, 1901 of which are parsimony informative. Overall, the branch lengths of all complex thalloids are shorter than those of outgroup taxa, except for the genus *Cyathodium*, which has longer branches than all other species of complex thalloids sequenced (Fig. 2).

The backbone branching order within the Marchantiopsida is: Blasiales (*Neohodgsonia* (Sphaerocarpales (*Lunularia* (Marchantiaceae, all other complex thalloids)))) (Fig. 2). The clade containing *Neohodgsonia* and the rest of the complex thalloids has a 100% MLB and 1.0 PP. The Sphaerocarpales (*Sphaerocarpos*, *Geothallus*, *Riella*, *Austroriella* and *Monocarpus*) are strongly supported (100% MLB, 1.0 PP). The clade containing *Lunularia* and the rest of Marchantiales is not as well supported (77% MLB, 0.99 PP). The clade containing Marchantiales is supported with 99% MLB, 1.0 PP, and most internal clades are highly supported (Fig. 2). Marchantiaceae (*Marchantia*, *Preissia* and *Bucegia*) are the earliest divergent members of Marchantiales, with high support (100% MLB, 1.0 PP). An accession comprising organellar genome sequences labeled *Marchantia polymorpha* from GenBank is sister to *M. paleacea* from Mexico. *Marchantia* itself is paraphyletic, with *Bucegia* and *Preissia* nested within. *Asterella* is also polyphyletic, whereas most other genera are monophyletic. *Dumortiera* is recovered as sister to most crown group complex thalloids, except Marchantiaceae, with high support (99% MLB, 1.0 PP). All orders are highly supported: Blasiales, Neohodgsoniales, Lunulariales, Sphaerocarpales and Marchantiales, the latter order containing most complex thalloid diversity (Fig. 2).

Molecular clock dating

Using the fossil and the secondary root calibration, the age of the complex thalloid crown group is 295 Ma (median age, HPD, 250–365 Ma) (Permian–Carboniferous, Fig. 3; Table 3; Fig. S1 for HPD values for all clades). The age of the Marchantiidae (excluding Blasiales) is 262 Ma (HPD, 226–327 Ma, pink distribution in Fig. 3). The crown ages of complex thalloid genera are mostly Cretaceous, with the major clades diverging before the K/T extinction, at 65 Ma (Fig. 3, orange line). The crown group of Sphaerocarpales is of Jurassic–Triassic origin, 169 Ma (HPD, 115–234 Ma), whereas the crown group of Marchantiales, which contains most of the diversity, started to diversify in nearly the same time period, 196 Ma (HPD, 157–251 Ma; yellow distribution in Fig. 3). The crown group of *Marchantia* (including *Preissia* and *Bucegia*) diverged at 126 Ma (HPD, 77–173 Ma; green distribution in Fig. 3), similar to the nested genus *Cyathodium*. The clade of *Marchantia polymorpha*, *M. paleacea* from Mexico and the GenBank '*Marchantia polymorpha*' organellar genomes is of Late Cretaceous–Paleogene origin, 44 Ma (HPD, 21–70 Ma; Fig. 3). *Marchantia polymorpha*, with three subspecies, diversified in the late Miocene, 5 Ma (HPD, 2–11 Ma) (Fig. 3). The crown group, comprising Ricciaceae and Oxymitraceae, diverged at 115 Ma (HPD, 80–156 Ma), whereas the most species-rich genus, *Riccia*, has a Paleocene age, 60 Ma (HPD, 36–87 Ma).

© 2015 Royal Botanic Garden Edinburgh
New Phytologist © 2015 New Phytologist Trust

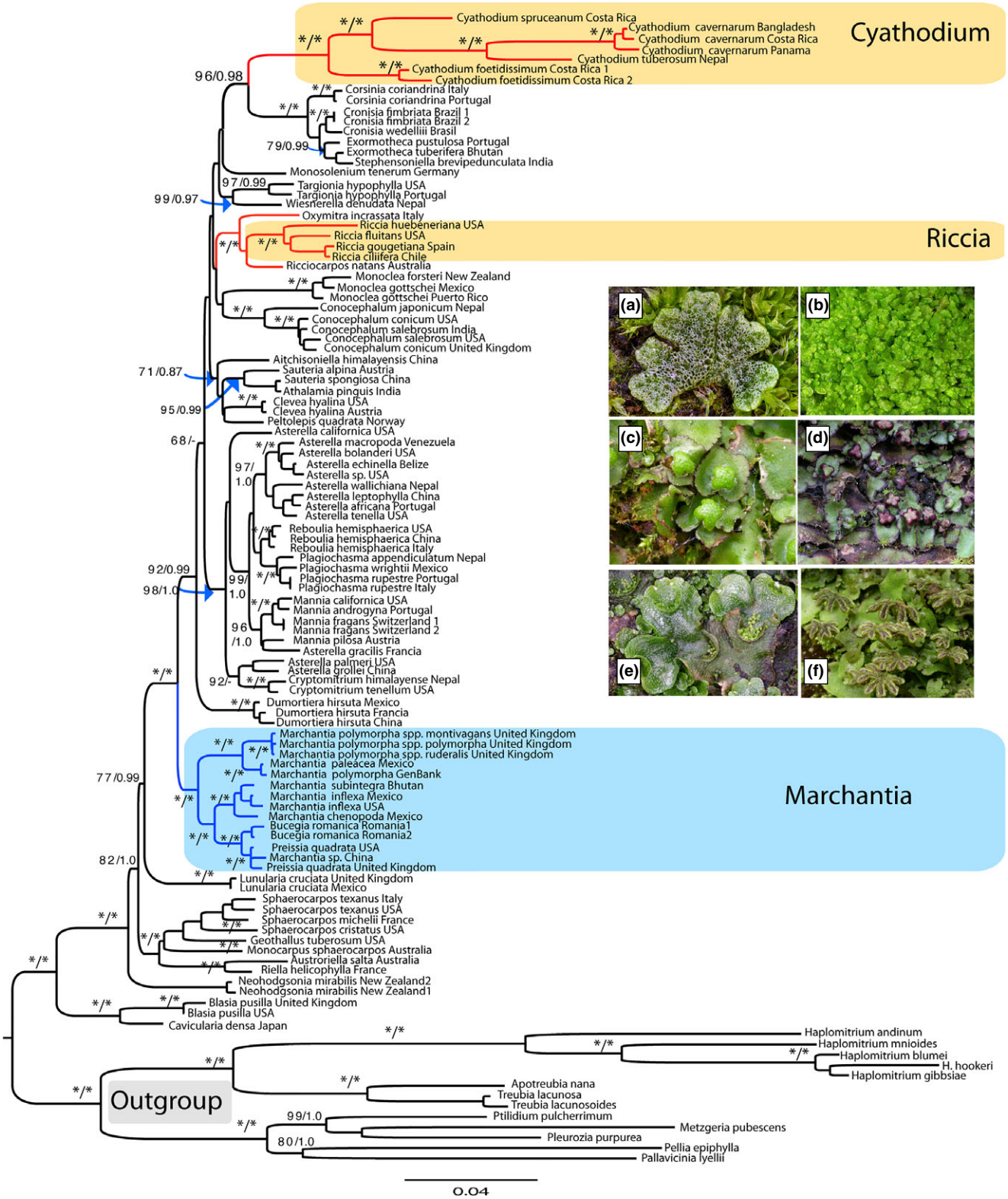

Fig. 2 Maximum likelihood tree for 98 accessions of complex thalloids and 13 outgroup taxa (from 14 829 aligned nucleotides of plastid, mitochondrial and nuclear ribosomal DNA). Maximum likelihood bootstrap values > 50% and < 100% are given, as are posterior probabilities over 0.95, whereas 100% bootstrap support and posterior probabilities of 1.0 are indicated with an asterisk. The genus *Marchantia* (blue box) contains the model species *M. polymorpha* comprising its three subspecies, *M. polymorpha* spp. *montivagans*, *polymorpha* and *ruderalis*, and also *Preissia* and *Bucegia*. The two genera with faster evolving lineages, *Riccia* and *Cyathodium*, are highlighted (orange boxes). Inset: exemplars of complex thalloid diversity: (a) *Riccia cavernosa*, (b) *Cyathodium* sp., (c) *Reboulia hemisphaerica*, (d) *Plagiochasma* sp., (e) *Lunularia cruciata* and (f) *Marchantia* sp. Credits (a, e) D. Callaghan; (b–d, f) Z. Li.

© 2015 Royal Botanic Garden Edinburgh
New Phytologist © 2015 New Phytologist Trust

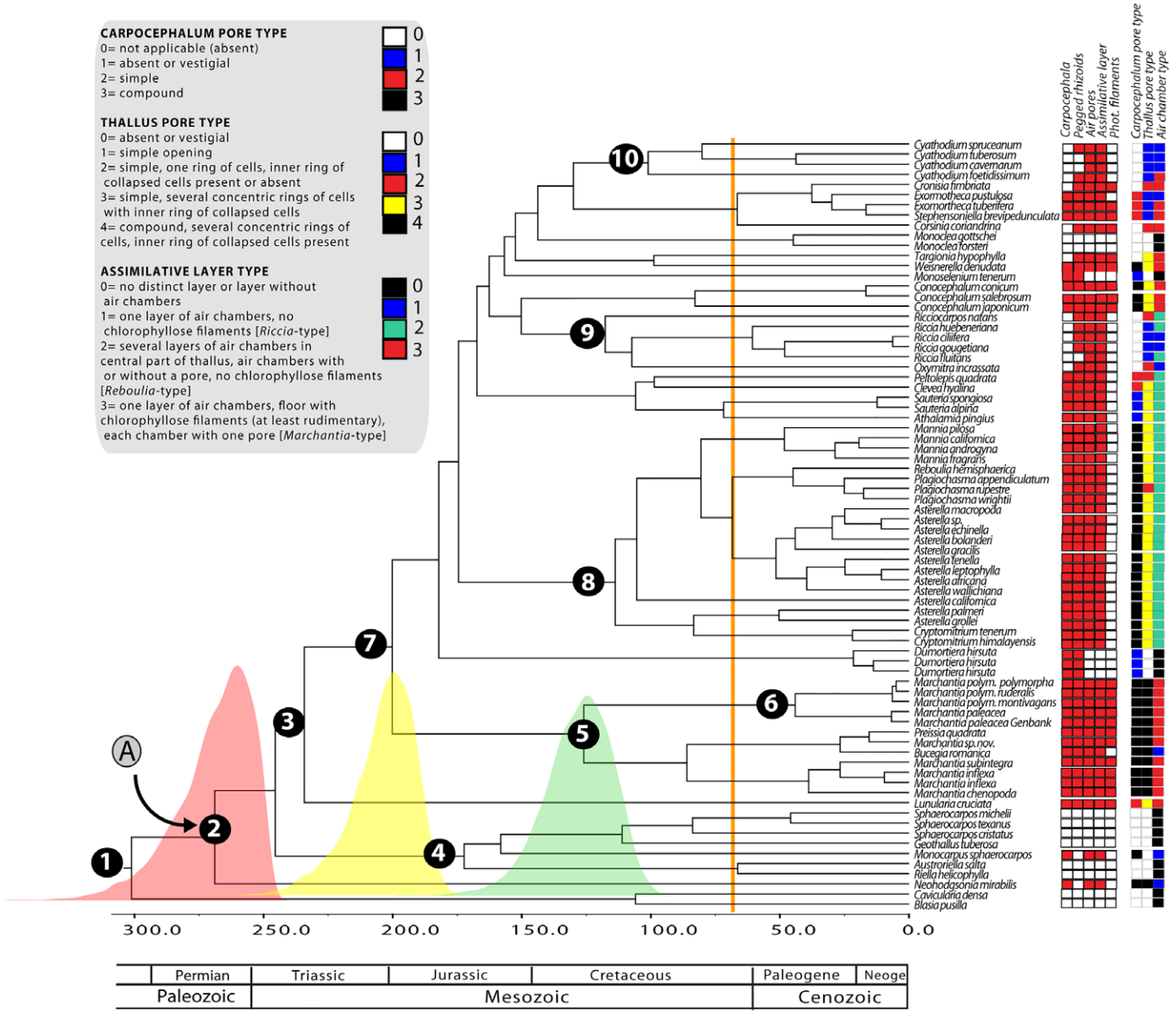

Fig. 3 Chronogram for complex thalloids, rooted on Blasiales, obtained from mitochondrial and plastid sequences modeled under a relaxed uncorrelated log-normal clock. Node heights represent mean ages; the 95% highest posterior density intervals for specific nodes are shown in Table 3 and Supporting Information Fig. S1. The distributions for three nodes are shown: node 2 (in pink, Marchantiidae); node 7 (in yellow, Marchantiales) and node 5 (in green, the genus *Marchantia sensu lato*). The letter A represents the calibration point, the Triassic fossil *Marchantites cyathoides* (see the Materials and Methods section). Numbers represent nodes of interest for dating analyses (Table 3) and for the ancestral character reconstruction (Table 2). To the right, each taxon has all five binary characters coded for presence (red) and absence (white). To the far right, three multistate characters are coded: carpocephalum pore type, thallus pore type and assimilative layer type. The coding scheme for each multistate character is shown in the upper left portion of the figure.

Rate heterogeneity

The absolute plastid mean substitution rate using the fossil and the secondary root calibration of the complex thalloids, including Blasiales, is 2.63×10^{-10} (SD, 0.0000046) substitutions per site per year. The absolute mitochondrial mean substitution rate of the complex thalloids is 5.31×10^{-11} (SD, 0.00000094) substitutions per site per year, with a faster rate for 26S, 7.76×10^{-10} (SD, 0.000014) substitutions per site per year. Bayesian analyses under UCLN and LC models yielded similar results and suggested one to two rate shifts. For UCLN analyses, the branches leading to *Cyathodium* are reconstructed as having higher relative rates of molecular evolution for all loci (Fig. S2). For example, the relative rate of the branch leading to Marchantiaceae is 0.274 (HPD, 0.11–0.51) and *Cyathodium* is 3.03 (HPD, 1.42–5.36). Using LC, the branch leading to Marchantiaceae is 0.795 (HPD, 0.11–0.51) and *Cyathodium* is 2.77 (HPD, 2.32–3.23), and up to 9.55 (HPD, 7.87–11.35) within the clade comprising *Cyathodium cavernarum*, *C. foetidissimum*, *C. spruceanum* and *C. tuberosum*

© 2015 Royal Botanic Garden Edinburgh
New Phytologist © 2015 New Phytologist Trust

Table 3 Divergence dates (in million years ago (Ma)) for the major complex thalloid clades (numbers in Fig. 3)

Nodes	1	2	3	4	5	6	7	8	9	10
Taxon	Marchantiopsida	Marchantidae	Lunulariales stem group	Sphaeorocarpales/ Riellales	Marchantiaceae	*Marchantia polymorpha – paleacea* crown group	Marchantiales crown group	Aytoniaceae crown group	*Ricciacea/ Oxymitraceae* crown group	*Cyathodium* crown group
Age (Ma)	**295.4** (HPD, 250.0–365.0)	**262.9** (HPD, 226.4–327.8.6)	**228.0** (HPD, 188.6–294.3)	**169.6** (HPD, 115.4–234.5)	**123.5** (HPD, 77.8–173.9)	**42.09** (HPD, 21.7–70.7)	**196.2** (HPD, 157.4–251.9)	**111.3** (HPD, 80.2–152.5)	**115.9** (HPD, 80.9–156.02)	**99.04** (HPD, 76.6–131.8)

Values in bold are median values of the age (in million years ago) of the crown group, with 95% posterior density intervals shown in parentheses.

(Fig. S3). The branch leading to *Riccia* has a slightly elevated rate of 0.85 (HPD, 0.11–2.10) (UCLN) and 1.00 (HPD, 0.78–1.88) (LC) for plastid loci. A similar pattern holds for mitochondrial and nuclear loci (data not shown).

Ancestral reconstruction of complex traits

Binary traits No significant difference was found between the one-rate and two-rate model with asymmetric rates (Tables 2, S3). Character reconstructions (Figs 3, S4–S8) show that air pores, an assimilative layer with air chambers and elevated carpocephala evolved after the splitting off of Blasiales, but before the divergence of *Neohodgsonia* (Fig. 3). Truly pegged rhizoids, however, did not evolve until after Sphaerocarpales diverged, but predate *Lunularia* (Fig. 3). All four characters have secondary losses: four for air pores (in the Sphaerocarpales, *Dumortiera*, *Monoclea* and *Monosolenium*); at least four for elevated carpocephala (Sphaerocarpales, *Riccia*/*Ricciocarpos*/*Oxymitra* clade, the ancestor of *Corsinia*/*Cronisia*/*Cyathodium*/*Monoclea* and in *Targionia*) and three or four for pegged rhizoids (Sphaerocarpales, *Cyathodium*, *Riccia fluitans* and *Monoclea*). The assimilative layer of air chambers is lost or vestigial in *Dumortiera*, *Monoclea* and *Monosolenium.* The ancestor of the complex thalloids lacked photosynthetic filaments; these first evolved after Sphaerocarpales diverged, but predate *Lunularia* (Fig. 3). Photosynthetic filaments have evolved at least four times in the Marchantiaceae (with a secondary loss in *Bucegia*), *Conocephalum*, *Exormotheca*/*Cronisia*/*Corsinia* and *Targionia*/*Weisnerella* (Fig. S8).

Multistate traits A simple pore with several concentric rings with an inner ring of collapsed cells (yellow in Fig. 3) evolved after Sphaerocarpales diverged, but predates *Lunularia*. The trait is ancestral to Marchantiales and is used as a defining trait of Aytoniaceae (yellow box in Fig. 3; Fig. S9). The more complex pore, compound with several concentric rings of cells and inner rings collapsed, evolved early in the complex thalloids. It is only found in the vegetative stage of Marchantiaceae and *Neohodgsonia*, although it is found on the carpocephalum of many taxa, including *Monocarpus*, *Conocephalum*, *Weisnerella*, Marchantiaceae and Aytoniaceae (black box in Fig. 3; Fig. S10). A simple opening is found in unrelated lineages, such as *Cyathodium*, Ricciaceae and *Exormotheca* (blue box in Fig. 3).

The assimilative layer type is ambiguous across the backbone of all complex thalloids (Figs 3, S11). The character combination of a single layer of air chambers with chlorophyllose filaments and each chamber with one pore arose independently in *Lunularia*, Marchantiaceae, *Conocephalum*, *Targionia*, *Weisnerella* and *Exormotheca*/*Cronisia*/*Corsinia* (red boxes in Fig. 3). A single layer of air chambers without chlorophyllose filaments occurs independently in *Cyathodium* and some *Riccia* (blue boxes in Fig. 3). The character combination of multiple layers of air chambers with or without pores and without filaments occurs once in the Aytoniaceae and also in *Ricciocarpos*, *Riccia* subgenus *Ricciella* and the *Clevea*/*Sauteria*/*Peltolepis* clade (green boxes in Figs 3, S11).

© 2015 Royal Botanic Garden Edinburgh
New Phytologist © 2015 New Phytologist Trust

Discussion

Our phylogeny (Fig. 2) cements the backbone topology of complex thalloid lineages, providing the phylogenetic framework required to assess evolutionary patterns of pegged rhizoids, carpocephala, air chambers, photosynthetic filaments and air pores. These five defining characters of the Marchantiidae presumably enabled radiations of complex thalloids into dry Mediterranean-type habitats, atypical of liverworts in general.

Phylogenetic relationships and rate of evolution

Previous phylogenies of complex thalloid liverworts showed low support for the main backbone relationships in the lineage (Wheeler, 2000; Boisselier-Dubayle *et al.*, 2002; Forrest *et al.*, 2006); our study confirms the monotypic genus *Neohodgsonia*, which has a uniquely branched carpocephalum, as the earliest divergent lineage of Marchantiidae (Fig. 2). The phylogenetic position of *Marchantia* is firmly supported in the earliest divergent lineage of the Marchantiales, but the genus is polyphyletic, with *Preissia* and *Bucegia* nested within it, as also shown by Boisselier-Dubayle *et al.* (2002) and Forrest *et al.* (2006). The position of *Dumortiera*, sister to the rest of Marchantiales (excluding Marchantiaceae), contrasts, however, with its strongly supported resolution within the crown group of Marchantiales, sister to *Monoclea*, in Forrest *et al.* (2006).

The strikingly low rate of molecular evolution in complex thalloids (Figs 1, 2) remains unexplained. The rate of plastid evolution in complex thalloids, 2.63×10^{-10} substitutions per site per year (Fig. 1a), is lower than that reported for other liverworts (9.0×10^{-10} substitutions per site per year, Feldberg *et al.*, 2014). The slow molecular rate in plastid and mitochondrial genomes for complex thalloids contrasts with a faster rate in the only ribosomal nuclear marker sequenced so far, ribosomal large subunit 26S (Wheeler, 2000; Boisselier-Dubayle *et al.*, 2002). Most factors used to explain the low rates in other lineages – for example, such as long generation time, large sizes and slow metabolism – are not easily quantifiable across liverworts or other bryophytes (Bromham, 2009; Korall *et al.*, 2010; Bromham *et al.*, 2015), although most liverworts are long lived to perennial.

There are two traits of complex thalloids that set them apart from the other liverwort clades: absence of RNA editing in organellar genes (Rüdinger *et al.*, 2012), which has typically been associated with a faster, not slower, substitution rate in other lineages (Mower *et al.*, 2007; Cuenca *et al.*, 2010), and the small size of their nuclear genomes (Bainard *et al.*, 2013). The average 1C genome size of complex thalloids is 0.654 ± 0.313 pg, in contrast with 6.085 ± 2.645 pg in Haplomitriopsida and 2.311 ± 3.811 pg in Jungermanniopsida (Table S4). However, the total number of genome size estimates for liverworts is currently too small (78 counts for *c.* 67 species; Temsch *et al.*, 2010; Bainard *et al.*, 2013) to be of statistical value.

The rate of evolution within complex thalloids is not constant (Figs 2, S2, S3). Although most lineages have notably slow rates of evolution, there are two exceptions: *Cyathodium* and, to a lesser extent, *Riccia*. Both have faster rates of evolution in both organellar and nuclear markers. *Cyathodium* is a largely tropical genus of 11 annual species (Salazar Allen, 2005), four of which are sampled here (*c.* 36%). *Riccia* is the most species-rich genus in the complex thalloids (*c.* 150 spp., four of which are sampled here – *c.* 3%), particularly diverse in Mediterranean regions (Bischler-Causse *et al.*, 2005). Many *Riccia* species are short-lived annuals, with *Riccia cavernosa*, with an Arctic growing season of 3–4 wk (Seppelt & Laursen, 1999), an extreme example. A correlation between a faster rate of molecular evolution and shorter generation time has been demonstrated in herbaceous angiosperms (Smith & Donoghue, 2008) and mammals (Bromham, 2009), and our results are consistent with shorter generation times as a factor leading to the longer branches in *Riccia* and *Cyathodium*. However, our severely limited sampling of *Riccia* species hampers a more rigorous examination of this phenomenon.

Divergence times, the origin of xerophyte taxa and the age of *Marchantia polymorpha*

The Cretaceous or Eocene origin of most complex thalloid genera reported here contrasts with the Miocene stem age of most other liverwort genera reported by Laenen *et al.* (2014) in a study that dated diversification across all liverworts, but had no fossil calibrations in the complex thalloid clade, and did not take into account their decelerated molecular rate. We believe that the younger ages reported by Laenen *et al.* (2014) are therefore misleading (see also Cooper *et al.*, 2012). Fossils with complex thalloid morphology have been well documented from Triassic and mid-Cretaceous sediments, supporting the ages recovered in our study (Anderson, 1976; Li *et al.*, 2014).

Many complex thalloid species are found in Mediterranean-type habitats and exhibit a xerophytic life style, with desiccation avoidance or tolerance strategies (e.g. *Corsinia*, *Exormotheca*, *Plagiochasma*, *Riccia*, *Targionia*; Vitt *et al.*, 2014), perhaps reflecting early diversification in adaptation to arid Triassic conditions (Wheeler, 2000). Our dated phylogeny supports a deep global divergence of these genera in the Cretaceous and early Tertiary, near the K/T global extinction (Fig. 3, orange line). Such xerophytic genera are notably absent from closed-canopy tropical rainforests (Bischler-Causse *et al.*, 2005), where other organisms, such as leptosporangiate ferns (Schuettpelz & Pryer, 2009), leafy liverworts and mosses (Feldberg *et al.*, 2014; Laenen *et al.*, 2014), experienced bursts of diversification. The most complete fossil data suggest that the angiosperm-dominated canopy spread after the K/T boundary global extinction, probably *c.* 56 Ma (Wing *et al.*, 2009), although molecular dating estimates of tropical plant groups placed the origin of tropical forest species in the Albian–Cenomanian (110 Ma) (Couvreur *et al.*, 2011). The divergence and diversification of xerophytic complex thalloids before 56 Ma suggests that they flourished in open areas before the closed angiosperm-dominated canopy spread.

Marchantia polymorpha is of very recent origin (late Miocene, 2–11 Ma). This age provides a minimum estimate for morphological evolution within the species and for the male chromosome in *Marchantia* (Yamato *et al.*, 2007). Dimorphic sex

© 2015 Royal Botanic Garden Edinburgh
New Phytologist © 2015 New Phytologist Trust

chromosomes in plants were first identified in *Sphaerocarpos donnellii* (Allen, 1917); if these are homologous with the *Marchantia* sex chromosomes, complex thalloid sex chromosomes may be the oldest among land plants (over 200 Ma), with potential to elucidate the evolution of sex-specific regions in embryophytes (Bowman, 2015).

Evolution of morphological complexity in Marchantiopsida

Ancestral state reconstructions suggest that a plant with a carpocephalum, with compound air pores present on the main thallus and on the carpocephalum, without pegged rhizoids, is the ancestral form for the Marchantiidae. Our results confirm morphological reductions in carpocephala and assimilatory layers and the re-evolution of complex suites of characters, such as air chambers with photosynthetic filaments, in nested lineages.

Carpocephalum

Stalked carpocephala are innovations that occur only within the complex thalloid liverworts (Marchantiidae) and are postulated to enhance wind dispersal of the very small spores found in many genera (Schuster, 1992). In the Jungermanniopsida and Haplomitriopsida, capsules (sporangia) are elevated above the gametophyte by auxin-mediated elongation of seta cells just before spore release, but, in most Marchantiopsida, seta elongation is highly reduced or even absent. Instead, sporophytes are elevated by the growth of a structurally modified gametophytic branch (the carpocephalum). Exceptions include the Blasiales and *Monoclea*, which both have jungermannioid-type seta elongation and lack carpocephala.

Carpocephala occur in *Neohodgsonia*, the first divergence of the Marchantiidae, and in most succeeding lineages, but are absent in all Sphaerocarpalean genera, except *Monocarpus*. Carpocephala are also absent in *Corsinia*, *Cronisia*, *Oxymitra*, *Riccia* and *Targionia* (Bischler, 1998), although sporophytes in *Oxymitra* are surrounded by a multi-layered photosynthetic involucre with pored air chambers (Sealey, 1930; Bischler, 1998), rather like a sessile carpocephalum. These taxa have reduced sporophytes, similar life history traits and very large spores that are released when the capsule and surrounding thallus deteriorate at the end of the growing season (Bischler, 1998). Some authors (e.g. Leitgeb, 1881) have argued that the lack of carpocephala is ancestral in Marchantiidae, but our data strongly support Goebel's hypothesis (Goebel, 1930) of secondary carpocephalum losses.

Pegged rhizoids

Pegged rhizoids, devoid of cytoplasm, are intimately involved in water transport in complex thalloids (Kamerling, 1897; Clee, 1943; Duckett *et al.*, 2014). Ontogenetically derived from smooth rhizoids, they are especially well developed in taxa in which water loss from the upper thallus is substantial (Goebel, 1905). In all taxa, vertically oriented, thin-walled smooth rhizoids, cytoplasmic at maturity, which anchor thalli to their substrates, form during early stages of sporeling or gemmaling growth. However, in most complex thalloids, as the plant matures, thicker walled, horizontal pegged rhizoids, dead at maturity, are also formed (Duckett *et al.*, 2014).

Our study indicates that the evolution of truly pegged rhizoids lagged behind the evolution of stalked receptacles. The early-diverging genus *Neohodgsonia*, with only smooth rhizoids, still exhibits dimorphism in rhizoid structure and orientation. In addition to its typical smooth rhizoids, there are smaller diameter, evenly thick-walled, dead at maturity rhizoids, seemingly functionally equivalent to the pegged rhizoids of more derived genera (Duckett *et al.*, 2014). These smaller smooth rhizoids are probably (given the phylogenetic placement of the lineage) the forerunners of pegged rhizoids, supporting the phylogenetic trend: all rhizoids smooth, alive (Blasiales, Sphaerocarpales) – rhizoids dimorphic, but all smooth, some large, alive and some small, dead (Neohodgsoniales) – rhizoids dimorphic with both smooth, alive and dead, pegged (most complex thalloid lineages). In derived lineages of Marchantiidae, pegged rhizoids are absent in only a few mesic taxa (e.g. *Monoclea*, some species of *Cyathodium* and *Riccia*; see Fig. 3).

The occurrence of dimorphic rhizoids in all lineages of the Marchantiidae, except Sphaerocarpales, suggests that dead-at-maturity, usually pegged, rhizoids are a fundamental character of the subclass, with an essential role in external water uptake and conduction along the ventral thallus surface. These horizontally oriented rhizoids, with associated ventral scales, can be internalized in rhizoid furrows in the specialized branches, or archegoniophores, which elevate the developing sporophyte receptacles (carpocephala). Although it appears that the pegged rhizoids in these furrows effectively conduct water (and sperm, at least in *Marchantia*; J. G. Duckett, pers. comm., 2015) through the archegoniophore, not all taxa have rhizoid furrows, including early-diverging *Monocarpus* and *Lunularia*, and later diverging *Plagiochasma* and *Athalamia*, although there are several genera with pegged rhizoids that do not produce elevated carpocephala.

Air chambers, pores and filaments

Like carpocephala, air chambers with pores are first found in *Neohodgsonia*, are absent in the Sphaerocarpales, except for *Monocarpus*, and present in most other lineages (Fig. 3). However, despite their similar early histories, losses of the two traits are not necessarily linked; for example, *Dumortiera* has rudimentary pore-less air chambers that lack overarching tissue, but has elevated female receptacles, as does *Monosolenium*. *Riccia* and *Ricciocarpos* lack carpocephala, but have thalli with well-developed, pored air chambers.

The morphology of complex thalloid air chambers is variable (Fig. 3). A one-layered air chamber without photosynthetic filaments (*Riccia*-type; Evans, 1918) evolved before *Neohodgsonia*, is lost in Sphaerocarpales (except *Monocarpus*) and is re-gained in only a few crown group lineages. The most complex air chambers, in which the chambers form a single layer and each chamber has abundant photosynthetic filaments arising from the chamber floor (Figs 1c, 3) (*Marchantia*-type; Evans, 1918), are found in

© 2015 Royal Botanic Garden Edinburgh
New Phytologist © 2015 New Phytologist Trust

Lunularia, the Marchantiaceae (except *Bucegia*) and a few scattered lineages in the crown group. Filament-less air chambers that occur in several layers (*Reboulia*-type) are found in almost all members of Aytoniaceae, and independently in some *Riccia* species and members of Cleveaceae.

Air chambers are generally associated with epidermal pores that range from being simple openings between unspecialized epidermal cells, as in *Riccia* subgenus *Riccia* and *Cyathodium*, to complex, elevated rings of cells that are either one (simple pores, e.g. *Lunularia*) or two (compound pores, e.g. *Marchantia*) cell layers thick at the pore itself (Bischler, 1998). Compound pores, developmentally more complicated than simple pores (Burgeff, 1943), are frequently found on carpocephala across the Marchantiidae, for example, in *Neohodgsonia*, *Monocarpus*, Marchantiaceae, Aytoniaceae, *Conocephalum* and *Wiesnerella*. However, only *Neohodgsonia* and Marchantiaceae also possess this pore type on the vegetative thallus (Fig. 3). In other lineages, thallus air chambers are associated with simple pores, an exception being *Dumortiera*, which has air chambers but lacks pores. Our results support the idea that compound air pores occurring on both thalli and carpocephala is ancestral in complex thalloids, with various types of simple pores derived.

Intercellular spaces connected to the atmosphere via openings or pores were a crucial innovation of land plants. *Marchantia*, as an easily cultured haploid plant, is a clear target in which to study the evolution of structures involved in gas exchange, aided by the recent knock-out of *NOPPERABO1* (*NOP1* gene), giving rise to a phenotype that failed to develop both schizogenous air chambers and pores (Ishizaki *et al.*, 2013a,b).

The character reconstructions in this study show that the defining characters of the Marchantiidae evolved deep within the complex thalloid lineage, first by the elevation of sex organs on highly modified upright gametophyte branches and the development of specialized gas exchange chambers within the gametophyte that connect schizogenous cavities to the atmosphere via specialized pores, and later by the addition of non-collapsing dead cells to conduct water up the upright branches. These structures have clear parallels in vascular plants, which have stomata and stomatal chambers for gas exchange, and dead-at-maturity cells that transport water along leaves and branches.

Acknowledgements

We are grateful for funding from the Scottish Government's Rural and Environment Science and Analytical Services Division and Sibbald Trust Grant 2014#17 to J.C.V., and National Science Foundation (NSF) grant EF-0531750 to B.J.C-S. Comments by three anonymous reviewers greatly improved the manuscript.

Author contributions

J.C.V. and L.L.F. planned and designed the research; J.C.V., L.L.F., D.G.L. and M.L.H. performed the experiments; D.G.L. and B.J.C-S. conducted the fieldwork; J.C.V. analyzed the data; J.C.V., L.L.F. and B.J.C-S. wrote the manuscript.

References

Allen CE. 1917. A chromosome difference correlated with sex differences in *Sphaerocarpos*. *Science, N.S.* **46**: 466–467.

Anderson HM. 1976. A review of the Bryophyta from the Upper Triassic Molteno Formation, Karroo Basin, South Africa. *Palaeontologia Africana* **19**: 21–30.

Bainard JD, Forrest LL, Goffinet B, Newmaster SG. 2013. Nuclear DNA content variation and evolution in liverworts. *Molecular Phylogenetics and Evolution* **68**: 619–627.

Barnes CR, Land WJG. 1907. Bryological papers. I. The origin of air chambers. *Botanical Gazette* **44**: 197–213.

Bischler H. 1998. Systematics and evolution of the genera of the Marchantiales. *Bryophytorum Bibliotheca* **51**: 1–201.

Bischler-Causse H, Gradstein SR, Jovet-Ast S, Long DG, Salazar Allen N. 2005. Marchantiidae. *Flora Neotropica Monographs* **97**: 1–267.

Boisselier-Dubayle MC, Lambourdiére J, Bischler H. 2002. Molecular phylogenies support multiple morphological reductions in the liverwort subclass Marchantiidae (Bryophyta). *Molecular Phylogenetics and Evolution* **24**: 66–77.

Bowman JL. 2015. A brief history of *Marchantia* from Greece to genomics. *Plant Cell and Physiology* **56**: doi: 10.1093/pcp/pcv044.

Bromham JL. 2009. Why do species vary in their rate of molecular evolution? *Biology Letters* **5**: 401–404.

Bromham L, Hua X, Lanfear R, Cowman PF. 2015. Exploring the relationships between mutation rates, life history, genome size, environment, and species richness in flowering plants. *American Naturalist* **185**: 507–524.

Brown RC, Lemmon BE, Shimamura M, Villarreal JC, Renzaglia KS. 2015. Spores of relictual bryophytes: diverse adaptations to life on land. *Review of Palaeobotany and Palynology* **216**: 1–17.

Burgeff H. 1943. *Genetische Studien an Marchantia*. Jena, Germany: Gustav Fischer.

Clee DA. 1943. The morphology and anatomy of *Fegatella conica* in relation to the mechanism of absorption and conduction of water. *Annals of Botany* **VII**: 185–193.

Cooper EE, Henwood MJ, Brown EA. 2012. Are the liverworts really that old? Cretaceous origins and Cenozoic diversifications in Lepidoziaceae reflect a recurrent theme in liverwort evolution. *Biological Journal of the Linnean Society* **107**: 425–441.

Couvreur TLP, Forest F, Baker WJ. 2011. Origin and global diversification patterns of tropical rain forests: inferences from a complete genus-level phylogeny of palms. *BMC Biology* **9**: 44.

Cuenca A, Petersen G, Seberg O, Davis JI, Stevenson DW. 2010. Are substitution rates and RNA editing correlated? *BMC Evolutionary Biology* **10**: 349.

Drummond AJ, Suchard MA. 2010. Bayesian random local clocks, or one rate to rule them all. *BMC Biology* **8**: 1–12.

Drummond AJ, Suchard MA, Xie D, Rambaut A. 2012. Bayesian phylogenetics with BEAUti and the BEAST 1.7. *Molecular Biology and Evolution* **29**: 1969–1973.

Duchêne S, Lanfear R, Ho SYW. 2014. The impact of calibration and clock-model choice on molecular estimates of divergence times. *Molecular Phylogenetics and Evolution* **78**: 277–289.

Duckett JG, Ligrone R, Renzaglia KS, Pressel S. 2014. Pegged and smooth rhizoids in complex thalloid liverworts (Marchantiopsida): structure, function and evolution. *Botanical Journal of the Linnean Society* **174**: 68–92.

Evans AW. 1918. The air chambers of *Grimaldia fragrans*. *Bulletin of the Torrey Botanical Club* **45**: 235–251.

Feldberg K, Schneider H, Stadler T, Schäfer-Verwimp A, Schmidt AR, Heinrichs J. 2014. Epiphytic leafy liverworts diversified in angiosperm-dominated forests. *Scientific Reports* **4**: 5974.

Forrest LL, Davis EC, Long DG, Crandall-Stotler BJ, Hollingsworth ML, Clark A. 2006. Unravelling the evolutionary history of the liverworts (Marchantiophyta) – multiple taxa, genomes and analyses. *The Bryologist* **109**: 303–334.

Goebel K. 1905. *Organography of plants, II. Special organography, 1st edn.* English translation by Balfour IB. Oxford, UK: Clarendon Press.

© 2015 Royal Botanic Garden Edinburgh
New Phytologist © 2015 New Phytologist Trust

Goebel K. 1930. *Organographie der Pflanzen, II. Bryophyten-Pteridophyten, 3rd edn*. Jena, Germany: Gustav Fischer.

Heinrichs J, Hentschel J, Wilson R, Feldberg K, Schneider H. 2007. Evolution of leafy liverworts (Jungermanniidae, Marchantiophyta), estimating divergence times from chloroplast DNA sequences using penalized likelihood with integrated fossil evidence. *Taxon* **56**: 31–44.

He-Nygren X, Ahonen I, Juslen A, Glenny D, Piippo S. 2004. Phylogeny of liverworts – beyond a leaf and a thallus. In: Goffinet B, Hollowell V, Magill MR, eds. *Molecular systematics of Bryophytes (MSB 98)*. St Louis, MO, USA: Missouri Botanical Garden Press, 87–118.

Ishizaki K, Johzuka-Hisatomi Y, Ishida S, Iida S, Kohchi T. 2013a. Homologous recombination-mediated gene targeting in the liverwort *Marchantia polymorpha* L. *Scientific Reports* **3**: 1532.

Ishizaki K, Mizutani M, Shimamura M, Masuda A, Nichihama R, Kohchi T. 2013b. Essential role of the E3 Ubiquitin Ligase NOPPERABO1 in schizogenous intercellular space formation in the liverwort *Marchantia polymorpha*. *Plant Cell* **25**: 4075–4084.

Kamerling Z. 1897. Zur Biologie und Physiologie der Marchantiaceen. *Flora* **84**: 1–68.

Katagiri T, Hagborg A. 2015. Validation of ordinal and family names for a Triassic fossil liverwort, *Naiadita* (Naiaditaceae, Marchantiopsida). *Phytotaxa* **222**: 165–166.

Korall P, Schuettpelz E, Pryer KM. 2010. Abrupt deceleration of molecular evolution linked to the origin of arborescence in ferns. *Evolution* **64**: 2786–2792.

Laenen B, Shaw B, Schneider H, Goffinet B, Paradis E, Désamoré A, Heinrichs J, Villarreal JC, Gradstein SR, McDaniel SF *et al.* 2014. Extant diversity of bryophytes emerged from successive post-Mesozoic diversification bursts. *Nature Communications* **5**: 6134.

Lanfear R, Calcott B, Ho SYW, Guindon S. 2010. Partitionfinder: combined selection of partitioning schemes and substitution models for phylogenetic analyses. *Molecular Biology and Evolution* **29**: 1695–1701.

Leitgeb H. 1881. *Untersuchungen über die Lebermoose VI. Die Marchantieen und Allgemeine Bermerkungen über Lebermoose*. Graz, Austria: Leuschner & Lubensky.

Lewis LA, Mishler BD, Vilgalys R. 1997. Phylogenetic relationships of the liverworts (Hepaticae), a basal embryophyte lineage inferred from nucleotide sequence data of the chloroplast gene rbcL. *Molecular Phylogenetics and Evolution* **7**: 377–393.

Li R, Sun B, Wang H, He Y, Yang G, Yan D, Lin Z. 2014. *Marchantites huolinhensis* sp. nov. (Marchantiales): a new fossil liverwort with gemma cups from the Lower Cretaceous of Inner Mongolia, China. *Cretaceous Research* **50**: 16–26.

Maddison WP, Maddison DR. 2010. *Mesquite: a modular system for evolutionary analysis, version 2.73*. [WWW document] URL http://mesquiteproject.org. [accessed 15 August 2015].

Miller MA, Holder MT, Vos R, Midford PE, Liebowitz T, Chan L, Hoover P, Warnow T. 2010. *The CIPRES Portals*. [WWW document] URL http://www.phylo.org [accessed 15 August 2015].

Mower JP, Touzet P, Gummow JS, Delph LS, Palmer JD. 2007. Extensive variation in synonymous substitution rates in mitochondrial genes of seed plants. *BMC Evolutionary Biology* **7**: 135.

Newton AE, Wikstrom N, Bell N, Forrest L, Ignatov MS, Tangney RS. 2007. Dating the diversification of the pleurocarpous mosses. In: Newton AE, Tangney RS, eds. *Pleurocarpous mosses, systematics and evolution*. Boca Raton, FL, USA: CRC Press, 337–366.

Oda K, Yamato K, Ohta E, Nakamura Y, Takemura M, Nozato N, Akashi K, Kanegae T, Ogura Y, Kohchi T *et al.* 1992. Gene organization deduced from the complete sequence of liverwort *Marchantia polymorpha* mitochondrial DNA. A primitive form of plant mitochondrial genome. *Journal of Molecular Biology* **223**: 1–7.

Ogg JG. 2012. Triassic. In: Gradstein FM, Ogg JG, Schmitz M, Ogg G, eds. *The geologic time scale 2012*. Boston, MA, USA: Elsevier, 681–730.

Ohyama K, Fukuzawa H, Kohchi T, Shirai H, Sano T, Sano S, Umesono K, Shiki Y, Takeuchi M, Chang Z *et al.* 1986. Chloroplast gene organization deduced from complete sequence of liverwort *Marchantia polymorpha* chloroplast DNA. *Nature* **322**: 572–574.

Pagel M. 1999. The maximum likelihood approach to reconstructing ancestral character states of discrete characters on phylogenies. *Systematic Biology* **48**: 612–622.

Parham JE, Donoghue PCJ, Bell CJ, Calway TD, Head JJ, Holroyd PA, Inoue JG, Irmis RB, Joyce WG, Ksepka DT *et al.* 2012. Best practices for justifying fossil calibrations. *Systematic Biology* **61**: 346–359.

Qiu YL, Libo L, Wang B, Chen Z, Knoop V, Groth-Malonek M, Dombrovska O, Lee J, Kent L, Rest J *et al.* 2006. The deepest divergences in land plants inferred from phylogenomic evidence. *Proceedings of the National Academy of Sciences, USA* **103**: 15511–15516.

Rambaut A. 2014. *Figtree: A graphical viewer of phylogenetic trees*. [WWW document] URL http://tree.bio.ed.ac.uk/software/ [accessed 15 August 2015].

Rambaut A, Suchard M, Drummond A. 2014. *Tracer, version 1.6.0*. [WWW document] URL http://tree.bio.ed.ac.uk/software/tracer/ [accessed 15 August 2015].

Ronquist F, Teslenko M, van der Mark P, Ayres DL, Darling A, Höhna S, Larget B, Liu L, Suchard MA, Huelsenbeck JP. 2012. MrBayes 3.2. Efficient Bayesian phylogenetic inference and model choice across a large model space. *Systematic Biology* **61**: 539–542.

Rüdinger M, Volkmar U, Lenz H, Groth-Malonek M, Knoop K. 2012. Nuclear DYW-type PPR gene families diversify with increasing RNA editing frequencies in liverwort and moss mitochondria. *Journal of Molecular Evolution* **74**: 37–51.

Saint-Marcoux D, Proust H, Dolan L, Langdale JA. 2015. Identification of reference genes for real-time quantitative PCR experiments in the liverwort *Marchantia polymorpha*. *PLoS ONE* **10**: 3.

Salazar Allen N. 2005. Cyathodium. In: Bischler-Causse H, Gradstein SR, Jovet Ast S, Long DG, Salazar Allen N, eds, *Marchantiidae. Flora Neotropica Monographs* **97**: 1–267.

Schuettpelz E, Pryer KM. 2009. Evidence for a Cenozoic radiation of ferns in an angiosperm-dominated canopy. *Proceedings of the National Academy of Sciences, USA* **106**: 11200–11205.

Schuster RM. 1992. *The Hepaticae and Anthocerotae of North America VI*. Chicago, IL, USA: Field Museum of Natural History.

Sealey JQ. 1930. The morphology of *Oxymitra androgyna*. *American Journal of Botany* **17**: 19–28.

Seppelt RD, Laursen A. 1999. *Riccia cavernosa* Hoffm. emend. Raddi, new to the Arctic and the bryoflora of Alaska. *Hikobia* **13**: 71–76.

Smith SA, Donoghue MJ. 2008. Rates of molecular evolution are linked to life history in flowering plants. *Science* **322**: 86–89.

Söderström L, Hagborg A, von Konrat M, Bartholomew-Began S, Bell D, Briscoe L, Brown E, Cargill DC, Costa DP, Crandall-Stotler BJ *et al.* (in press). World checklist of hornworts and liverworts. *Phytokeys*. doi: 10.3897/phytokeys.@.6261.

Stamatakis A, Hoover P, Rougemont J. 2008. A rapid bootstrap algorithm for the RAxML web-servers. *Systematic Biology* **75**: 758–771.

Temsch E, Greilhuber J, Krisai R. 2010. Genome size in liverworts. *Preslia* **82**: 63–80.

Townrow JA. 1959. Two Triassic bryophytes from South Africa. *Journal of South African Botany* **25**: 1–22.

Vitt DH, Crandall-Stotler B, Wood AJ. 2014. Bryophytes, survival in a dry world through tolerance and avoidance. In: Rajakaruna N, Boyd RS, Harris TB, eds. *Plant ecology and evolution in harsh environments*. New York, NY, USA: Nova Science, 267–295.

Warnock RCM, Yang Z, Donoghue PCJ. 2012. Exploring uncertainty in the calibration of the molecular clock. *Biology Letters* **8**: 156–159.

Wellman CH, Osterloff PL, Mohiuddin U. 2003. Fragments of the earliest land plants. *Nature* **425**: 282–285.

Wheeler JA. 2000. Molecular phylogenetic reconstructions of the Marchantioid liverwort radiation. *The Bryologist* **103**: 314–333.

Wicket NJ, Mirarab S, Nguyen N, Warnow T, Carpenter E, Matasci N, Ayyampalayam S, Barker MS, Burleigh JG, Gitzendanner MA *et al.* 2014. A phylotranscriptomic analysis of the origin and early diversification of land plants. *Proceedings of the National Academy of Sciences, USA* **111**: E4859–E4868.

Wing L, Herrera F, Jaramillo CA, Gómez-Navarro C, Wilfe P, Labandeira CC. 2009. Late Paleocene fossils from the Cerrejon Formation, Colombia, are the earliest record of Neotropical rainforest. *Proceedings of the National Academy of Sciences, USA* **106**: 18627–18632.

© 2015 Royal Botanic Garden Edinburgh
New Phytologist © 2015 New Phytologist Trust

Yamato KT, Ishizaki K, Fujisawa M, Okada S, Nakayama S, Fujishita M, Bando H, Yodoya K, Hayashi K, Bando T *et al.* 2007. Gene organization of the liverwort Y chromosome reveals distinct sex chromosome evolution in a haploid system. *Proceedings of the National Academy of Sciences, USA* **104**: 6472–6477.

Supporting Information

Additional supporting information may be found in the online version of this article.

Fig. S1 Chronogram for complex thalloids, rooted on Blasiales, obtained from mitochondrial and plastid sequences modeled under a relaxed uncorrelated log-normal clock (see the Materials and Methods section).

Fig. S2 A comparison of the molecular clocks and their relative rates using uncorrelated log-normal (UCLN) analyses (see the Materials and Methods section).

Fig. S3 A comparison of the molecular clocks and their relative rates using a random local clock (LC) molecular clock analysis (see the Materials and Methods section).

Fig. S4 Chronogram for 76 species of complex thalloids with maximum likelihood ancestral reconstruction of carpocephalum.

Fig. S5 Chronogram for 76 species of complex thalloids with maximum likelihood ancestral reconstruction of rhizoid dimorphism.

Fig. S6 Chronogram for 76 species of complex thalloids with maximum likelihood ancestral reconstruction of air pores.

Fig. S7 Chronogram for 76 species of complex thalloids with maximum likelihood ancestral reconstruction of assimilative layers.

Fig. S8 Chronogram for 76 species of complex thalloids with maximum likelihood ancestral reconstruction of photosynthetic filaments.

Fig. S9 Chronogram for 76 species of complex thalloids with maximum parsimony ancestral reconstruction of carpocephalum pore types.

Fig. S10 Chronogram for 76 species of complex thalloids with maximum parsimony ancestral reconstruction of thallus air pore types.

Fig. S11 Chronogram for 76 species of complex thalloids with maximum parsimony ancestral reconstruction of air chamber types.

Table S1 List of species used in this study including authorities, localities, herbarium vouchers and GenBank accession numbers for all sequences.

Table S2 PCR conditions for all loci used in this study.

Table S3 Log-likelihoods associated with the reconstruction of trait evolution for two competing explicit evolutionary models (see text for details) in complex thalloids.

Table S4 Genome sizes and species diversity across liverworts.

Please note: Wiley Blackwell are not responsible for the content or functionality of any supporting information supplied by the authors. Any queries (other than missing material) should be directed to the *New Phytologist* Central Office.

© 2015 Royal Botanic Garden Edinburgh
New Phytologist © 2015 New Phytologist Trust